PHYSICAL REVIEW B **80**, 241402(R) (2009)

Dynamical response functions and collective modes of bilayer graphene

Giovanni Borghi,[1] Marco Polini,[2,*] Reza Asgari,[3] and A. H. MacDonald[4]
[1]*International School for Advanced Studies (SISSA), via Beirut 2-4, I-34014 Trieste, Italy*
[2]*NEST-CNR-INFM and Scuola Normale Superiore, I-56126 Pisa, Italy*
[3]*School of Physics, Institute for Research in Fundamental Sciences, IPM 19395-5531 Tehran, Iran*
[4]*Department of Physics, University of Texas at Austin, Austin, Texas 78712, USA*
(Received 3 September 2009; published 3 December 2009)

Bilayer graphene (BLG) has recently attracted a great deal of attention because of its electrically tunable energy gaps and its unusual electronic structure. In this Rapid Communication we present analytical and semianalytical expressions, based on the four-band continuum model, for the layer-sum and layer-difference density-response functions of neutral and doped BLG. These results demonstrate that BLG density fluctuations can exhibit either single-component massive-chiral character or standard two-layer character, depending on energy and doping.

DOI: 10.1103/PhysRevB.80.241402 PACS number(s): 71.10.−w, 71.45.Gm, 73.21.−b

I. INTRODUCTION

Recent progress[1] in the isolation and experimental exploration of large area single and multilayer graphene systems has opened up a new topic in two-dimensional electron system (2DES) physics. These atomically thin 2DESs exhibit a rich variety of unique properties that are presently under active investigation. In particular, the peculiarities of one single-layer graphene (SLG), two bilayer graphene (BLG),[2–5] and three layer systems are quite distinct. This Rapid Communication is motivated by ongoing experimental work on suspended BLG (Ref. 6) and improved BLG samples on SiC.[7] We anticipate that electron-electron interactions will have a crucial influence on the emerging Fermi liquid, collective excitation, angle-resolved photoemission spectroscopy (ARPES),[7] and tunneling properties of BLG systems.

Many-body effects in BLG have been studied by several authors.[8–14] However density-response functions, which are the starting point for detailed many-body physics considerations in charged-particle systems, have so far been calculated[12] only in the static limit, only in the density-density channel (see below), and only within a two-band model[15] whose applicability is limited to low densities and low energies. Dynamical screening and collective effects in BLG are still largely unexplored.

In this Rapid Communication we present analytical expressions based on the full four-band continuum model for the dynamical susceptibilities of undoped BLG and semianalytical expressions for the same quantities in doped BLG. Our results provide the key technical ingredient necessary for many-body theory calculations that are based on the random-phase approximation (RPA) (Ref. 16) or its generalizations, whether directed toward thermodynamic quantities (like charge and spin susceptibilities) or toward quasiparticle dynamics.[2,7] They exhibit many interesting features which foreshadow key aspects of many-body correlation physics in these systems. In the present Rapid Communication we present detailed RPA predictions for the collective plasmon excitations of BLG, which are expected to be directly observable in electron energy loss spectroscopy studies and, as in the SLG case, are responsible for the many-body features observable in ARPES spectra.[17,18]

II. FOUR-BAND LINEAR-RESPONSE THEORY

BLG is modeled as two SLG systems separated by a distance d and coupled by both interlayer hopping and Coulomb interactions. Most of the properties we discuss below depend qualitatively on the Bernal stacking arrangement in which one sublattice (say A) of the top layer is a near neighbor of the opposite sublattice (say B) of the bottom layer. Neglecting trigonal warping, which is important only at extremely low densities and is presently masked by uncontrolled disorder, the single-particle Hamiltonian is ($\hbar=1$) $\hat{\mathcal{T}}=\sum_{\boldsymbol{k},\alpha,\beta}\hat{c}^{\dagger}_{\boldsymbol{k},\alpha}\mathcal{T}_{\alpha\beta}(\boldsymbol{k})\hat{c}_{\boldsymbol{k},\beta}$, where $\mathcal{T}(\boldsymbol{k})=-v\gamma^5\gamma^0\gamma\cdot\boldsymbol{k}-t_\perp(\gamma^5\gamma^x+i\gamma^y)/2$. Here v ($\sim 10^6$ m/s) is the Fermi velocity of an isolated graphene layer, $t_\perp$ (~ 0.3 eV) is the interlayer hopping amplitude, and the γ^μ are 4×4 Dirac γ matrices in the chiral representation[19] ($\gamma^5\equiv -i\gamma^0\gamma^1\gamma^2\gamma^3$). The Greek indices α,β account for the sublattice degrees of freedom in top ($1=A$, $2=B$) and bottom ($3=A$, $4=B$) layers. Two electrons in the same (S) layer interact via the 2D Coulomb potential $V_S(q)=2\pi e^2/(\epsilon q)$. Electrons in different (D) layers interact via $V_D(q)=V_S(q)\exp(-qd)$.

For response function calculations it is convenient to work in the single-particle Hamiltonian eigenstate basis. Diagonalization of $\mathcal{T}(\boldsymbol{k})$ yields four hyperbolic bands[8] (see Fig. 1) with dispersions, $\varepsilon_{1,2}(\boldsymbol{k})=\pm\sqrt{v^2k^2+t_\perp^2/4}+t_\perp/2$ and $\varepsilon_{3,4}(\boldsymbol{k})=\pm\sqrt{v^2k^2+t_\perp^2/4}-t_\perp/2$. In this basis the interaction contribution to the Hamiltonian is $\hat{\mathcal{H}}_{\rm int}=(2S)^{-1}\sum_{\boldsymbol{q}}[V_+(q)\hat{\rho}_{\boldsymbol{q}}\hat{\rho}_{-\boldsymbol{q}}+V_-(q)\hat{\Upsilon}_{\boldsymbol{q}}\hat{\Upsilon}_{-\boldsymbol{q}}]$, where S is the 2DES area, $V_\pm=(V_S\pm V_D)/2$, and $\hat{\rho}_{\boldsymbol{q}}$ and $\hat{\Upsilon}_{\boldsymbol{q}}$ are respectively the operators for the sum and difference of the individual layer densities: $\hat{\rho}_{\boldsymbol{q}}=\sum_{\boldsymbol{k},\lambda,\lambda'}\hat{c}^{\dagger}_{\boldsymbol{k}-\boldsymbol{q},\lambda}(\mathcal{D}_{\boldsymbol{k}-\boldsymbol{q},\boldsymbol{k}})_{\lambda\lambda'}\hat{c}_{\boldsymbol{k},\lambda'}$ with $\mathcal{D}_{\boldsymbol{k}-\boldsymbol{q},\boldsymbol{k}}=\mathcal{U}^{\dagger}_{\boldsymbol{k}-\boldsymbol{q}}\mathcal{U}_{\boldsymbol{k}}$ and $\hat{\Upsilon}_{\boldsymbol{q}}=\sum_{\boldsymbol{k},\lambda,\lambda'}\hat{c}^{\dagger}_{\boldsymbol{k}-\boldsymbol{q},\lambda}(\mathcal{S}_{\boldsymbol{k}-\boldsymbol{q},\boldsymbol{k}})_{\lambda\lambda'}\hat{c}_{\boldsymbol{k},\lambda'}$ with $\mathcal{S}_{\boldsymbol{k}-\boldsymbol{q},\boldsymbol{k}}=\mathcal{U}^{\dagger}_{\boldsymbol{k}-\boldsymbol{q}}\gamma^5\mathcal{U}_{\boldsymbol{k}}$. Here $\mathcal{U}_{\boldsymbol{k}}$ is the unitary transformation from sublattice to band labels λ,λ'.[8] From $\hat{\mathcal{H}}_{\rm int}$ we thus see that two response functions are necessary for the evaluation of collective modes and ground-state properties of BLG: the total-density-response function, $\chi_{\rho\rho}(q,\omega)=\langle\langle\hat{\rho}_{\boldsymbol{q}};\hat{\rho}_{-\boldsymbol{q}}\rangle\rangle_\omega/S$, and the density-difference response function $\chi_{\rm YY}(q,\omega)=\langle\langle\hat{\Upsilon}_{\boldsymbol{q}};\hat{\Upsilon}_{-\boldsymbol{q}}\rangle\rangle_\omega/S$. Here $\langle\langle\hat{A};\hat{B}\rangle\rangle_\omega$ is the Kubo product.[20,22]

III. NONINTERACTING RESPONSE FUNCTIONS AND RPA SCREENING

In the noninteracting limit the linear-response functions introduced above have the standard eigenstate-representation form,[20]

$$\chi^{(0)}_{\rho\rho(\mathrm{YY})} = \sum_{\lambda,\lambda'} \int \frac{d^2\boldsymbol{k}}{(2\pi)^2} \frac{n_{\boldsymbol{k},\lambda} - n_{\boldsymbol{k}',\lambda'}}{z + \Delta_{\boldsymbol{k},\lambda;\boldsymbol{k}',\lambda'}} \mathcal{M}_{\boldsymbol{k},\lambda;\boldsymbol{k}',\lambda'}, \tag{1}$$

where $z=\omega+i0^+$, $\boldsymbol{k}'=\boldsymbol{k}+\boldsymbol{q}$, $n_{\boldsymbol{k},\lambda}$ are band occupation factors, and $\Delta_{\boldsymbol{k},\lambda;\boldsymbol{k}',\lambda'}=\varepsilon_{\boldsymbol{k},\lambda}-\varepsilon_{\boldsymbol{k}',\lambda'}$ are band-energy differences. Here $\mathcal{M}_{\boldsymbol{k},\lambda;\boldsymbol{k}',\lambda'}$ is $|(\mathcal{D}_{\boldsymbol{k},\boldsymbol{k}'})_{\lambda\lambda'}|^2$ for the total-density response and $|(\mathcal{S}_{\boldsymbol{k},\boldsymbol{k}'})_{\lambda\lambda'}|^2$ for the density-difference response. We have evaluated $\chi^{(0)}_{\rho\rho(\mathrm{YY})} \to \chi^{(0\mathrm{u})}_{\rho\rho(\mathrm{YY})}$ analytically for undoped BLG, i.e., for the case in which bands 2 and 4 are full and bands 1 and 3 are empty. Here we report only results for the imaginary parts of these response functions. The corresponding analytical expressions for the real parts, which can be derived from a standard Kramers-Krönig analysis, are extremely cumbersome and will be presented elsewhere. After very lengthy algebra we have reached the following results (per spin and per valley):

$$\Im m\chi^{(0\mathrm{u})}_{\rho\rho}(q,\omega) = \left\{ \frac{1}{16v^2}\left[\frac{v^2f^2(q,\omega) - 2v^2q^2}{\sqrt{g(q,\omega,\omega)}} + 2\sqrt{g(q,\omega,\omega)} - \frac{2}{\omega}|g(q,\omega,\omega_-)| \right]\Theta(g(q,\omega,\omega) - t_\perp^2) \right.$$
$$\left. - \frac{1}{8v^2\omega}[\omega\sqrt{g(q,\omega_-,\omega_-)} - |g(q,\omega,\omega_-)|]\Theta(g(q,\omega_-,\omega_-) - t_\perp^2) \right\} + \left\{ \cdots \right\}_{t_\perp \to -t_\perp} \tag{2}$$

and

$$\Im m\chi^{(0\mathrm{u})}_{\mathrm{YY}}(q,\omega) = \left\{ \frac{1}{16v^2}\left[\frac{v^2f^2(q,\omega_-) - 2v^2q^2 - 2t_\perp^2}{\sqrt{g(q,\omega_-,\omega_-)}} + 2\sqrt{g(q,\omega_-,\omega_-)} - \frac{2}{\omega}|g(q,\omega,\omega_-)| \right]\Theta(g(q,\omega_-,\omega_-) - t_\perp^2) \right.$$
$$\left. - \frac{1}{8v^2\omega}[\omega\sqrt{g(q,\omega,\omega)} - |g(q,\omega,\omega_-)|]\Theta(g(q,\omega,\omega) - t_\perp^2) \right\} + \left\{ \cdots \right\}_{t_\perp \to -t_\perp}, \tag{3}$$

where $\omega_\pm=\omega\pm t_\perp$, $g(q,\omega,\Omega)=\omega\Omega-v^2q^2$, $f(q,\omega)=q\sqrt{[g(q,\omega,\omega)-t_\perp^2]/g(q,\omega,\omega)}$, and $\Theta(x)$ is the usual step function. Equations (2) and (3) greatly simplify the analysis of many-body effects in BLG and are an important result of this work.

For both density-sum and density-difference channels, the response functions of the *doped* system can be written as $\chi^{(0)}=\chi^{(0\mathrm{u})}+\delta\chi^{(0)}$. We find that the corrections due to doping can be reduced to simple but cumbersome one-dimensional (1D) integrals,[21]

$$\delta\chi^{(0)}_{\rho\rho(\mathrm{YY})}(q,z) = \left\{ \Theta(\varepsilon_\mathrm{F} - t_\perp)\frac{1}{4\pi v}\int_{t_\perp/(2v)}^{\varepsilon_\mathrm{F}/v - t_\perp/(2v)} [g_{\rho\rho(\mathrm{YY})}(s,q,z,t_\perp) + j_{\rho\rho(\mathrm{YY})}(s,q,z,-t_\perp)]ds \right.$$
$$\left. + \frac{1}{4\pi v}\int_{t_\perp/(2v)}^{\varepsilon_\mathrm{F}/v + t_\perp/(2v)} [g_{\rho\rho(\mathrm{YY})}(s,q,z,-t_\perp) + j_{\rho\rho(\mathrm{YY})}(s,q,z,t_\perp)]ds \right\} + \left\{ \cdots \right\}_{z\to -z}, \tag{4}$$

where

$$g_{\rho\rho} = \frac{-[v^2q^2 - a(z)a(z_+)]^2\mathrm{sgn}(\Re e[P(q,z)])}{[a^2(z_+) - z^2]\sqrt{Q(q,z)}} + \frac{R(q)}{4[a^2(z_+) - z^2]} - \frac{5}{4} - \frac{z_-}{4(s + t_\perp/2)}, \tag{5}$$

$$j_{\rho\rho} = \mathrm{sgn}(\Re e[P(q,z_-)])\frac{\sqrt{Q(q,z_-)}}{a^2(z_-) - z^2} - \frac{R(q)}{4[a^2(z_-) - z^2]} + \frac{1}{4} + \frac{z_-}{4(s - t_\perp/2)}, \tag{6}$$

$$g_{\mathrm{YY}} = \mathrm{sgn}(\Re e[P(q,z)])\frac{\sqrt{Q(q,z)}}{a^2(z_+) - z^2} - \frac{R(q)}{4[a^2(z_+) - z^2]} + \frac{1}{4} + \frac{z_-}{4(s + t_\perp/2)}, \tag{7}$$

and

$$j_{\mathrm{YY}} = \frac{-[v^2q^2 + t_\perp z - a^2(z_-)]^2\mathrm{sgn}(\Re e[P(q,z_-)])}{[a^2(z_-) - z^2]\sqrt{Q(q,z_-)}} + \frac{R(q)}{4[a^2(z_-) - z^2]} - \frac{5}{4} - \frac{z_-}{4(s - t_\perp/2)}. \tag{8}$$

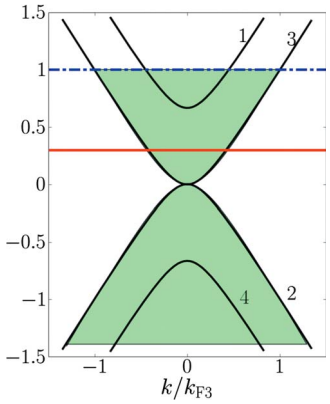

FIG. 1. (Color online) BLG continuum-model band structure. Depending on the doping level, the 2DES can have either one or two conduction-band Fermi surfaces.

Here $z_{\pm}=z\pm t_{\perp}$, $a(z)=z+2vs$, $P(q,z)=v^2q^2-za(z)$, $Q(q,z)=v^4q^4+a^2(z)z^2+q^2[t_{\perp}^2-a^2(z)-z^2]$, and $R(q)=|4v^2q^2+t_{\perp}^2-4v^2s^2|$. Note that the first term inside the curly brackets in Eq. (4) is finite only if the high-energy band $\varepsilon_1(\boldsymbol{k})$ is occupied (i.e., only if the Fermi energy $\varepsilon_F>t_{\perp}$). Equations (4)–(8) constitute the second important result of this work.

The static limit of these response functions $\chi^{(0)}_{\rho\rho(\mathrm{YY})}(q,\omega=0)$ is illustrated in Fig. 2 for both lightly and heavily doped bilayers.[23] In the low-density limit $\chi^{(0)}_{\rho\rho}(q,0)$ exhibits a strong Kohn anomaly at $q=2k_{F3}$ associated with[12] the massive-chiral behavior of band 3 at energies below $\sim t_{\perp}$. We see in Fig. 2 that response functions calculated in the two-band model[12] (dashed line in Fig. 2) overestimate the strength of this nonanalyticity because they do not capture the gradual change in the single-particle eigenstate character of band 3 from the coherent two-layer wave functions at low energies to weakly coupled SLG wave functions at high energies. For

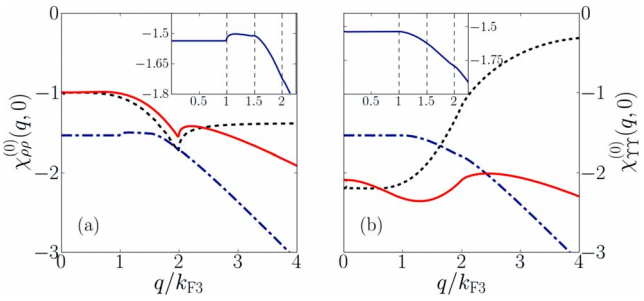

FIG. 2. (Color online) BLG static response in units of the Fermi-level density of states of band 3, $\nu=(\varepsilon_F+t_{\perp}/2)/(2\pi v^2)$, as a function of q/k_{F3}. (a) $\chi^{(0)}_{\rho\rho}(q,0)$. The (black) dashed line is the result obtained within the two-band model (Ref. 12), while the (red) solid line is the result obtained within the four-band model for doping level $n=10^{12}$ cm^{-2}, corresponding to the (red) solid line in Fig. 1. The (blue) dash-dotted line gives the static response for $n=5\times10^{13}$ cm^{-2} corresponding to the (blue) dash-dotted line in Fig. 1. Inset: small momenta region of the heavily doped result. From left to right, the vertical dashed lines are at $2k_{F1}$, $k_{F1}+k_{F3}$, and $2k_{F3}$. (b) $\chi^{(0)}_{YY}(q,0)$ with the same labeling as in panel (a). The two-band model $\chi^{(0)}_{YY}(q,0)$ reported here has been calculated with a cutoff $k_c=t_{\perp}/v$.

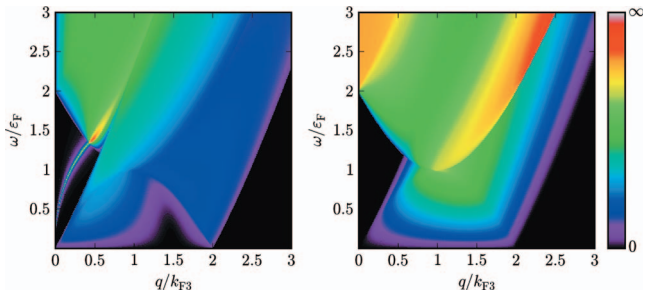

FIG. 3. (Color) BLG RPA dynamical dielectric functions for low-doping $n=10^{12}$ cm^{-2} and $\alpha_{ee}=0.5$. The left panel shows $\Im m[1/\varepsilon_{\rho\rho}(q,\omega)]$ as a function of q (in units of k_{F3}) and ω (in units of ε_F). The right panel shows $\Im m[1/\varepsilon_{YY}(q,\omega)]$.

the same reason the two-band model completely misrepresents the large-q behavior, failing to capture the linear increase in $\chi^{(0)}$ at large q which closely mimics SLG behavior. In the high-density limit $\chi^{(0)}_{\rho\rho}(q,0)$ becomes rather similar to its SLG counterpart. The Kohn anomaly at $2k_{F1}$, which still has BLG character at this energy, is relatively strong while the anomaly at $2k_{F3}$, which already has more single-layer character, is strongly suppressed. The real-space Friedel oscillations (FOs) exhibit corresponding changes[24] as the occupation of band 1 increases at high densities. In panel b we clearly see that the two-band model is even more inadequate in the density-difference channel. (In fact the integrals which appear in $\chi^{(0)}_{YY}(q,0)$ have an ultraviolet divergence[25] in the two-band model.) $\chi^{(0)}_{YY}$ is larger than $\chi^{(0)}_{\rho\rho}$ at small q for low densities because of the two-layer character wave functions are easily polarized. At higher densities $\chi^{(0)}_{YY}$ and $\chi^{(0)}_{\rho\rho}$ are nearly identical, as expected when the two layers respond nearly independently.

IV. RPA THEORY OF COLLECTIVE MODES

The RPA response functions of the interacting doped system are given by

$$\chi_{\rho\rho(\mathrm{YY})}=\frac{\chi^{(0)}_{\rho\rho(\mathrm{YY})}}{1-V_{\pm}\chi^{(0)}_{\rho\rho(\mathrm{YY})}}\equiv\frac{\chi^{(0)}_{\rho\rho(\mathrm{YY})}}{\varepsilon_{\rho\rho(\mathrm{YY})}}. \tag{9}$$

The interacting-system susceptibilities are determined by the density n, d (which we have taken to be $d=3.35$ Å), $t_{\perp}$

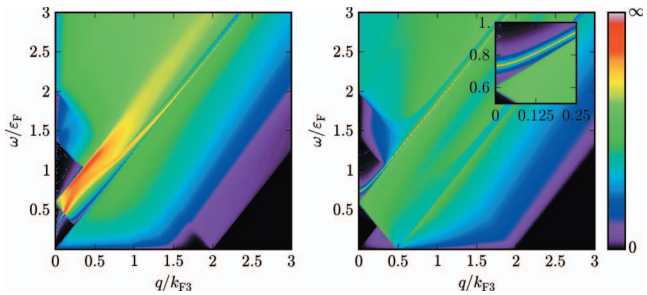

FIG. 4. (Color) High density ($n=5\times10^{13}$ cm^{-2}) BLG RPA dynamical dielectric functions for the same model parameters as in Fig. 3. The inset in the right panel highlights the intersubband plasmon.

(which we have taken to be 0.35 eV), and by the effective fine-structure constant $\alpha_{ee}=e^2/(\hbar v \epsilon)$. In Figs. 3 and 4 we plot the imaginary parts, $\Im m[1/\varepsilon_{\rho\rho}(q,\omega)]$ and $\Im m[1/\varepsilon_{YY}(q,\omega)]$, of the inverse dynamic dielectric functions which provide a portrait of BLG density-sum and density-difference fluctuations and collective modes. The collective fluctuation physics in the high-density limit is much like that of an ordinary bilayer,[26] as expected. A clear in-phase bilayer plasmon, whose frequency goes to zero such as $\sqrt{q}$ for $q \to 0$ appears at low energies and is Landau damped at relatively low frequencies by interband transitions. An out-of-phase intersubband plasmon appears in $\varepsilon_{YY}(q,\omega)$ just above the transition frequency between bands 3 and 1. At low densities, however, these results show that the collective fluctuation physics in BLG is quite unusual. The intersubband plasmon is Landau damped at all wavevectors for $\varepsilon_F < t_\perp/2$, i.e., for densities below $n_c=3(t_\perp/v)^2/(4\pi)\sim 7\times 10^{12}$ cm^{-2}, which is smaller than the critical density $n_1=2(t_\perp/v)^2/\pi \sim 18\times 10^{12}$ cm^{-2} at which the band $\varepsilon_1(\boldsymbol{k})$ is populated. The density-sum plasmon still appears and still has $\sqrt{q}$ dispersion but the physics which determines the coefficient of $\sqrt{q}$ is completely altered.[27] The shark-fin structure around $\omega=0$ and $q=\sqrt{2}k_{F3}$ inside the *e-h* continuum is a direct consequence of the $J=2$ massive-chiral fermion behavior because it leads to suppressed scattering from a state with momentum $\boldsymbol{k}$ to a state with final momentum $(\boldsymbol{k}+\boldsymbol{q}) \perp \boldsymbol{k}$. The disappearance of the intersubband plasmon in $\Im m[1/\varepsilon_{YY}(q,\omega)]$ occurs because the mode would be Landau damped even if strong, and because long-wavelength transition amplitudes between bands 1 and 3 are suppressed at low energies.

In summary we have demonstrated that the density-sum and density-difference fluctuations in BLG crossover from those of an unusual massive-chiral single-layer system to those of a weakly coupled bilayer as carrier density, wave vector, and energy increase. The analytic and semianalytic results for RPA response functions obtained here will simplify efforts to understand the many-body physics of this unique 2DES.

ACKNOWLEDGMENTS

G.B. and M.P. acknowledge M. Gibertini and F. Poloni for very useful discussions. M.P. acknowledges partial financial support from the CNR-INFM "Seed Projects" and very inspiring conversations with Eli Rotenberg. Work in Austin was supported by the NSF under Grant No. DMR-0606489.

*m.polini@sns.it

[1] A. H. Castro Neto *et al.*, Rev. Mod. Phys. **81**, 109 (2009).
[2] T. Ohta *et al.*, Science **313**, 951 (2006).
[3] K. S. Novoselov *et al.*, Nat. Phys. **2**, 177 (2006).
[4] E. V. Castro *et al.*, Phys. Rev. Lett. **99**, 216802 (2007).
[5] J. B. Oostinga *et al.*, Nature Mater. **7**, 151 (2008).
[6] J. Martin, Bull. Am. Phys. Soc. **54**, 191 (2009); B. Feldman *et al.*, arXiv:0909.2883, Nat. Phys. (to be published).
[7] E. Rotenberg (private communication).
[8] J. Nilsson *et al.*, Phys. Rev. B **73**, 214418 (2006).
[9] X.-F. Wang and T. Chakraborty, Phys. Rev. B **75**, 041404(R) (2007).
[10] H. Min *et al.*, Phys. Rev. B **77**, 041407(R) (2008).
[11] S. V. Kusminskiy *et al.*, Phys. Rev. Lett. **100**, 106805 (2008); S. Viola Kusminskiy *et al.*, EPL **85**, 58005 (2009).
[12] E. H. Hwang and S. Das Sarma, Phys. Rev. Lett. **101**, 156802 (2008).
[13] G. Borghi *et al.*, Solid State Commun. **149**, 1117 (2009).
[14] C. Toke and V. Fal'ko, arXiv:0903.2435 (unpublished).
[15] E. McCann and V. I. Fal'ko, Phys. Rev. Lett. **96**, 086805 (2006).
[16] RPA is of course not exact. It should be viewed as a good starting point to analyze the collective behavior of charged many-particle systems. Its use in graphene away from the neutrality point is partly justified. For perturbative treatments of interactions in bilayer graphene it is the fine-structure constant α_{ee}, rather than the density as in a normal 2D electron gas, which acts as a small parameter. The value of this parameter, which just depends on the dielectric environment surrounding BLG, is quite small ($\sim$0.5) for samples deposited on SiO_2 or grown on SiC.
[17] A. Bostwick *et al.*, Nat. Phys. **3**, 36 (2007).
[18] M. Polini *et al.*, Phys. Rev. B **77**, 081411(R) (2008).
[19] M. Maggiore, *A Modern Introduction to Quantum Field Theory* (Oxford University Press, Oxford, 2005).
[20] G. F. Giuliani and G. Vignale, *Quantum Theory of the Electron Liquid* (Cambridge University Press, Cambridge, 2005).
[21] A key step in the derivation of these results is to remove nonanalyticities that stem from the four-band dispersions $\varepsilon_{\boldsymbol{k},\lambda}$ of BLG, which contain square roots and thus produce algebraic branch cuts that complicate the integrations in the complex plane. This was accomplished by considering *pairs* of terms in such a way to cancel contributions coming from branch cuts with opposite signs. Finally, even though the 1D integrals over the variable s in Eq. (4) could be performed analytically, it turns out that it is much more convenient to use these implicit expressions for numerical calculations. Indeed, they can be straightforwardly used to perform the analytical continuation to the real frequency axis.
[22] The mixed sum and difference response functions vanish because the system Hamiltonian is invariant under spatial inversion.
[23] The model's particle-hole symmetry guarantees that electron-doped and hole-doped bilayers have identical properties.
[24] G. Borghi, M. Polini, R. Asgari, and A. H. MacDonald (unpublished).
[25] The two-band model interband contribution to $\chi^{(0)}_{YY}$ is $\propto \int dkk \cos^2(\varphi_{\boldsymbol{k},\boldsymbol{k}+\boldsymbol{q}})/(\varepsilon_{\boldsymbol{k}}+\varepsilon_{\boldsymbol{k}+\boldsymbol{q}}) \propto \int^{k_c} dkk(1/k^2) \propto \ln(k_c)$. Here $\varphi_{\boldsymbol{k},\boldsymbol{k}+\boldsymbol{q}}$ is the angle between $\boldsymbol{k}$ and $\boldsymbol{k}+\boldsymbol{q}$, $\varepsilon_{\boldsymbol{k}}=\hbar^2k^2/(2m^\star)$ with $m^\star=t_\perp/(2v^2)$, and the integrand has been expanded for $k\to\infty$.
[26] S. Das Sarma and E. H. Hwang, Phys. Rev. Lett. **81**, 4216 (1998); S. H. Abedinpour *et al.*, *ibid.* **99**, 206802 (2007).
[27] M. Polini *et al.*, arXiv:0901.4528 (unpublished).